Monthly Notices
of the
ROYAL ASTRONOMICAL SOCIETY

MNRAS **491,** 2953–2958 (2020)
Advance Access publication 2019 November 12

doi:10.1093/mnras/stz3144

Radiative lifetimes, branching fractions, and oscillator strengths of high-lying levels in Re I

Yongfan Li,[1]★ Sébastien Gamrath,[2] Patrick Palmeri,[2] Pascal Quinet,[2,3]★ Qiu Li,[1] Qi Yu,[1] Meiqi Zhang,[1] Lina Zhou[1] and Zhenwen Dai[1]★

[1]*Key Laboratory of Physics and Technology for Advanced Batteries (Ministry of Education), College of Physics, Jilin University, Changchun 130012, China*
[2]*Physique Atomique et Astrophysique, Université de Mons, B-7000 Mons, Belgium*
[3]*IPNAS, Université de Liège, B-4000 Liège, Belgium*

Accepted 2019 November 6. Received 2019 November 1; in original form 2019 July 24

ABSTRACT

Radiative lifetimes of 19 levels in Re I were measured using the time-resolved laser-induced fluorescence method. As far as we know, 15 results are reported for the first time. By combining the experimental lifetimes determined from this work with theoretical branching fractions obtained by a pseudo-relativistic Hartree–Fock model including core-polarization contributions, a new set of semi-empirical transition probabilities and oscillator strengths for 47 Re I lines from 18 newly measured levels were derived.

Key words: atomic data – atomic processes – methods: laboratory: atomic – techniques: spectroscopic.

1 INTRODUCTION

The interest of radiative parameters of heavy neutron-capture (n-capture) elements is mainly due to their importance in astrophysics. Radiative parameters, including radiative lifetimes, branching fractions (BFs), transition probabilities, and oscillator strengths are of great significance to determine the chemical abundance, which allow understanding of the *s* (slow) and *r* (rapid) processes in the buildup of heavy-nuclei nucleosynthesis (Fivet et al. 2006a). Besides, reliable radiative parameters are also particularly useful in studies of stars with temperatures and atmospheres different from the Sun (Wickliffe, Lawler & Nave 2000). Over the years, radiative parameter determinations have been performed for some heavy n-capture elements, such as Ta I (Li et al. 2019), Os II (Quinet et al. 2006), Ir I (Zhou et al. 2018), and Au II (Fivet et al. 2006b). However, there is no sufficient work focused on the neutral rhenium (Re I). Therefore, in this paper, we aim to the determination of radiative parameters for Re I, which has been observed in the chemically peculiar stars, e.g. in 73 Dra (Guthrie 1972) and in HD 25 354 (Jaschek & Brandi 1972).

The energy levels of Re I were compiled by Moore (1958) with $5d^5 6s^2\ a^6S_{5/2}$ as the ground state. Experimental oscillator strengths of Re I were first reported by Corliss and Bozman (1962). Later on, in 1982, with the method of the time-resolved laser-induced fluorescence (TR-LIF), Duquette, Salih & Lawler (1982) measured lifetimes of nine levels for Re I with which the improved oscillator strengths were determined by combining the BFs derived from Corliss and Bozman's transition probability data (Corliss & Bozman 1962). Using the same method, in 2006, radiative lifetimes of 11 odd-parity levels of Re I were measured by Palmeri et al. (2006). They also presented semi-empirical transition probabilities for 81 Re I lines by combining experimental lifetimes with their theoretical BFs calculated with the Hartree–Fock-plus-relativistic-corrections (HFR) method (Palmeri et al. 2006). In 2012, using the laser-induced breakdown spectroscopy, Ortiz and Mayo-García (2012) measured oscillator strengths of 30 Re I lines, 26 of which were reported for the first time.

Until now, to the best of our knowledge, only 19 lifetimes of Re I levels were reported in the literature. Considering the needs in astrophysics, in this paper, we measured new radiative lifetimes of 19 Re I odd-parity levels lying in the range 32 591.63–47 970.82 cm^{-1} by TR-LIF method and 15 of them were reported for the first time. In addition, the lifetimes of the 18 levels reported in this work were combined with our theoretical BFs obtained by the HFR method including core-polarization effects to derive semi-empirical transition probabilities (*gA*) and oscillator strengths (log(*gf*)) for 47 Re I lines.

2 LIFETIME MEASUREMENTS

In this paper the lifetimes were measured by TR-LIF method, whose reliability has stood the test of time (Fivet et al. 2006b; Quinet et al. 2009; Zhang, Feng & Dai 2010; Tian et al. 2016). The experimental setup has been described in details previously (Zhang et al. 2011), so here is just a brief reminder.

The rhenium plasma was obtained by laser ablation in a vacuum chamber. The ablation pulses were produced by a 532 nm Q-

★ E-mail: 1365394881@qq.com (YL); pascal.quinet@umons.ac.be (PQ); dai@jlu.edu.cn (ZD)

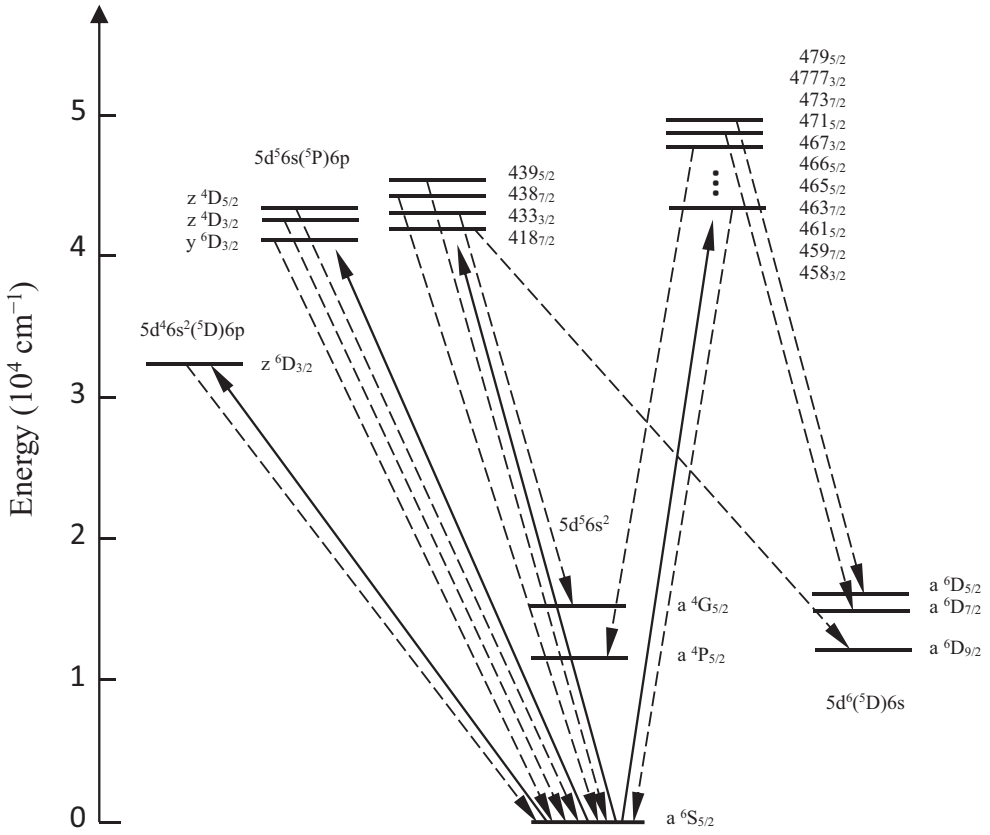

Figure 1. Energy level diagram of Re I. The solid lines indicate the excitation pathways, while the dashed lines indicate the observed fluorescence.

switched Nd: YAG laser with the energy of 10–20 mJ, a 10 Hz repetition rate, and about 8 ns pulse duration. A multiple-range tunable laser was used to excite the Re atoms from lower states to the aimed states selectively. It can be a DCM dye laser which was inspired by another 532 nm Q-switched Nd: YAG laser with 10 Hz repetition rate and about 10 ns pulse width, the second or third harmonics waves of this dye laser by one or two β-barium borate (BBO) type-I crystals, or be their Raman shift laser produced through a hydrogen cell (Zhang et al. 2018). The dye laser had a 0.08 cm^{-1} linewidth and an about 6 ns pulse duration. The fluorescence from the aimed upper level was collected by a fused silica lens into a grating monochromator with a photomultiplier tube (PMT, Hamamatsu R3896), and finally recorded and averaged by an oscilloscope (Tektronix DPO7254). The directions of the ablation laser, the excitation laser, and the fluorescence collection were perpendicular to each other. The delay time between the excitation and ablation pulses can be tuned from 1 to 100 μs by a digital delay generator (DG535), which can also be helpful to avoid most effects such as collision effect and saturation effect etc. More details about how to check and eliminate the effects influencing measurements can be found in our previous papers (Shang et al. 2014).

In the lifetime measurements, the single-step excitation scheme was utilized. A diagram for the relevant energy levels and transitions of Re I is shown in Fig. 1. The channels of excitation and fluorescence detection were carefully chosen or checked for avoiding possible co-excitation and blending. To get satisfactory signal-to-noise ratio, each fluorescence curve at different delay times was averaged with more than 1000 shots. Typical decay curves of the 42 254.19 and 32 591.63 cm^{-1} levels in Re I are shown in Figs 2 and 3. In Fig. 2, the lifetime result was obtained by a convolution fitting, while in Fig. 3 an exponential fitting was used. One can see that the signal-to-noise ratios and the fittings are satisfactory.

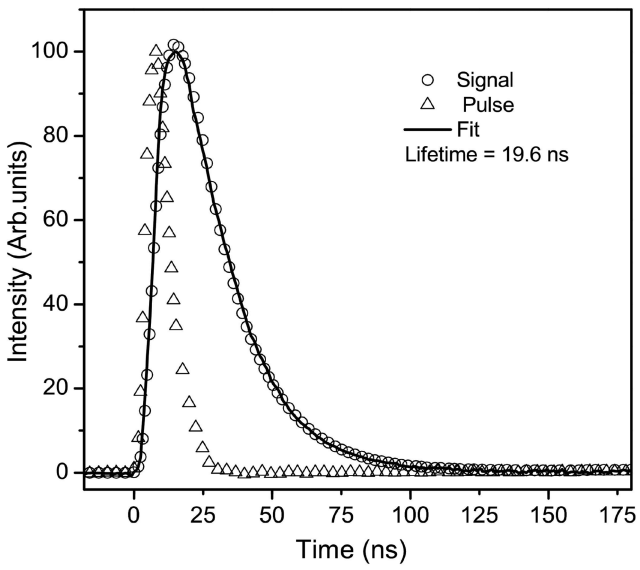

Figure 2. Typical fluorescence decay curve of the 42 254.19 cm^{-1} level of Re I with a convolution fit.

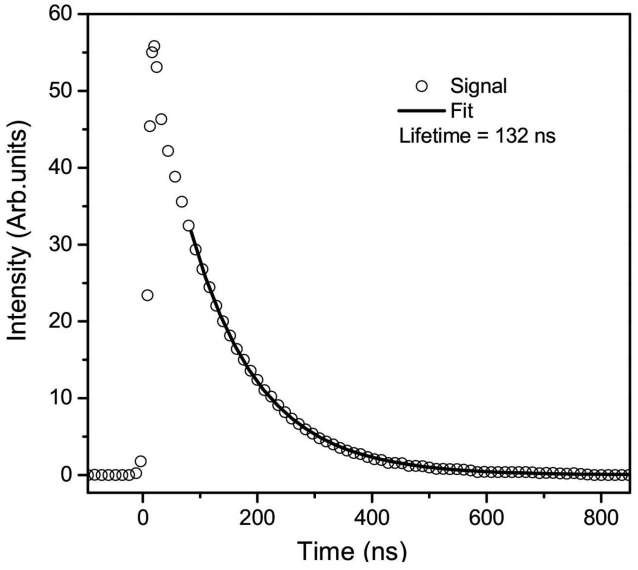

Figure 3. Typical fluorescence decay curve of the 32 591.63 cm^{-1} level of Re I with an exponential fit.

3 CALCULATIONS OF BRANCHING FRACTIONS

The theoretical model used in this work for computing the radiative rates and the corresponding branching fractions (BF) in Re I is exactly the same as in Palmeri et al. (2006). More precisely, the pseudorelativistic HFR method of Cowan (1981) was chosen as both relativistic and correlation effects must be taken simultaneously into account in the calculation of the atomic structure of such a heavy element as rhenium ($Z = 75$). The relativistic corrections were incorporated as the mass-velocity, one-body Darwin, and Blume–Watson spin-orbit terms. The latter term comprises the part of the Breit interaction that can be reduced to a one-body operator (Blume & Watson, 1962, 1963). This approach was modified as described by Quinet et al. (Quinet et al. 1999; Quinet et al. 2002) in order to take into account the core–polarization effects leading to the HFR+CPOL method. In that framework, the core–valence correlation was included implicitly by considering a $5d^4$ Re IV ionic core surrounded by three valence electrons. In addition, a value of 6.81 au for the ionic core dipole polarizability was taken from Fraga, Karwowski & Saxena (1976) while the cut-off radius adopted was the HFR mean radius of the 5d orbit in the Re I ground configuration, i.e. 1.87 au. On the other hand, the valence–valence correlation was incorporated explicitly through the superposition of the following interacting configurations: $5d^6ns$, $5d^56sns$, $5d^7$, $5d^66d$, $5d^56s6d$, $5d^46s^26d$, $5d^56p^2$ and $5d^46s6p^2$ ($n = 6$–8) in the even parity and $5d^6np$, $5d^56snp$, $5d^46s^26p$, and $5d^46p^3$ ($n = 6$–8) in the odd parity. The missing interactions with far configurations not considered explicitly by the configuration interaction (CI) expansion or implicitly by the polarization model were taken into account in a first step through the down scaling by a factor of 0.8 of all the radial Coulomb parameters according to a well-established procedure (Cowan 1981). In a second step, the HFR+CPOL method was combined with a least-square optimization routine minimizing the discrepancies between the Hamiltonian eigenvalues and the experimental energy levels available in the literature (Klinkenberg 1957; Wyart 1978). The standard deviations were 88 and 176 cm^{-1} for respectively the even- and the odd-parity levels. In the fitting procedure, we included 54 even-parity levels below 36 000 cm^{-1} and 97 odd-parity levels below 50 000 cm^{-1}. They belong to the $5d^66s$, $5d^56s^2$, $5d^7$, $5d^66p$, $5d^56s6p$, and $5d^46s^26p$ configurations. From the 107 odd-parity levels below 50 000 cm^{-1} that were published by Klinkenberg et al. (1957), ten levels, i.e. 44 148.45, 47 779.91, 47 970.82, 48 857.60, 49 027.85, 49 286.07, 49 540.96, 49 573.11, 49 863.22, and 49 895.57 cm^{-1}, were in fact excluded from the fit because they caused the radial parameters to take unphysical values, or did not correspond to Hamiltonian eigenvalues. This was the case for the level at 47 779.91 cm^{-1} measured in this study. It is worth noting that Klinkenberg et al. (1957) did not assign any configuration to these levels.

Finally, the theoretical branching fractions (BF_{ki}) have been determined for each depopulating transition of the measured upper levels from the corresponding HFR+CPOL Einstein coefficients (A_{ki}) and HFR+CPOL lifetimes (τ_k) as follows:

$$BF_{ki} = A_{ki}\tau_k.$$

4 RESULTS AND DISCUSSION

The radiative lifetimes of 19 Re I levels measured in this work are presented in Table 1. These results are in the range of 9.9 to 132 ns with the measurement uncertainties from 2.8 to 10.2 per cent. The uncertainties were derived from the combination of statistical scattering errors and some systematic errors. See our previous paper (Shang et al. 2015) for more details. As far as we know, the results of 15 levels were experimentally measured for the first time, while the other four levels had also been measured by Palmeri et al. (2006). In Table 1 we also give their results for comparison. Our results of three levels at 32 591.63, 42 254.19, and 43 044.02 cm^{-1} are in very good agreement with their values. For the level 41 557.08 cm^{-1}, our result is 31.8 ± 0.7 ns while theirs is 36 ± 3 ns. Palmeri et al. (2006) pointed out that for this level a wrong correspondence between calculated and observed level cannot be ruled out. However, our experimental result is consistent with their calculated value 30.6 ns.

In this table, we also report the HFR+CPOL lifetimes computed in this work for comparison. One has to bear in mind that carrying out accurate calculations in such a complex heavy neutral atom as Re I with large number of overlapping configurations is challenging. In Re I, strong configuration interaction is also present for the low-lying levels (Palmeri et al. 2006) and it is even more so for the high-lying ones measured in this study as illustrated in Table 2. The major *LS* components are of the order of 20 per cent or even less. This has consequences on the calculation of the line strengths of depopulating channels and therefore on the corresponding theoretical lifetimes. One of these is the strong cancellation effects on the line strengths with small cancellation factors (CF < 0.05) as defined by Cowan (1981), i.e. the destructive interference caused by the representation of atomic states involved in the radiative transitions by superpositions of basis states. They lead to overestimated calculated lifetimes. In Table 1, the HFR+CPOL values affected by this effect are marked by an asterisk. The other one is the sensitivity of the radiative rates or lifetimes to small admixture coefficients that can be detected through the sensitivity to the fitting procedure. For instance, the level at 41 843.85 cm^{-1} has an HFR+CPOL lifetime of 23.6 ns after the fit and an *ab initio* value (i.e. before the fit) of 96.7 ns. Similar situations of high fit sensitivity were also encountered for other 12 levels among the calculated 18 ones, i.e. located at 32 591.63, 41 557.08, 42 254.19, 43 044.02, 43 949.98, 45 876.34, 45 937.18, 46 112.24, 46 352.99, 46 509.40, 46 733.38, and 47 101.61 cm^{-1}. This illustrates again the high difficulty to

Table 1. Measured lifetimes for Re I levels and comparison with present calculations and previous results. All the levels were excited from the ground state. The number in parentheses is the uncertainty in the last one or two digits of the reported result.

Upper Level[a]				Lifetime (ns)			
Assignment	E (cm^{-1})	$\lambda_{Exc.}$ (nm)	$\lambda_{Obs.}$ (nm)	Experiment		Calculation	
				This work	Previous	This work	Previous
$5d^46s^2(^5D)6p\ z\ ^6D^\circ_{3/2}$	32 591.63	306.827	460.241	132(8)	134(10)[b]	114	114[b]
$5d^56s(^5P)6p\ y\ ^6D^\circ_{3/2}$	41 557.08	240.633	360.950	31.6(15)	36(3)[b]	30.6	30.6[b]
$418^\circ_{7/2}$	41 843.85	238.984	498.516	77.3(26)	–	23.6	–
$5d^56s(^5P)6p\ z\ ^4D^\circ_{3/2}$	42 254.19	236.663	354.995	19.6(8)	19.0(15)[b]	37.1*	–
$5d^56s(^5P)6p\ z\ ^4D^\circ_{5/2}$	43 044.02	232.32	348.48	28.3(8)	30(2)[b]	65.0*	–
$433^\circ_{3/2}$	43 341.85	230.724	522.278	38.9(15)	–	84.7*	–
$438^\circ_{7/2}$	43 815.01	228.232	342.348	18.9(7)	–	15.7	–
$439^\circ_{5/2}$	43 949.98	227.531	341.297	9.9(7)	–	20.9*	–
$458^\circ_{3/2}$	45 876.34	217.977	326.966	38.2(16)	–	7.28	–
$459^\circ_{7/2}$	45 937.18	217.689	326.534	12.6(10)	–	12.4	–
$461^\circ_{5/2}$	46 112.24	216.862	325.293	10.4(6)	–	9.40	–
$463^\circ_{7/2}$	46 352.99	215.736	323.604	21.4(9)	–	17.3	–
$465^\circ_{5/2}$	46 509.40	215.01	322.515	20.5(10)	–	11.0	–
$466^\circ_{5/2}$	46 649.42	214.365	321.548	15.7(9)	–	10.5	–
$467^\circ_{3/2}$	46 733.38	213.98	320.97	18.0(6)	–	8.28	–
$471^\circ_{5/2}$	47 101.61	212.307	422.325	16.2(6)	–	40.6*	–
$473^\circ_{7/2}$	47 358.36	211.156	452.604	41.6(17)	–	38.7	–
$4777^\circ_{3/2}$	47 779.91	209.293	468.611	31.0(30)	–	–†	–
$479^\circ_{5/2}$	47 970.82	208.46	312.69	24.5(25)	–	26.3	–

Notes. [a]Kramida et al. (2018).
[b]Palmeri et al. (2006).
*Affected by strong cancellation effects on the line strengths of main contributions (see the text).
†Level excluded from the fitting procedure (see Palmeri et al. 2006 and the text).

Table 2. LS composition and comparison between experimental and calculated level energies and Landé factors, g, for the Re I odd-parity energy levels for which lifetime measurements were performed in this work.

E_{exp} (cm^{-1})[a]	E_{cal} (cm^{-1})[b]	J	g_{exp}[a]	g_{cal}[b]	LS composition[b,c]
32 591.63	32 817	3/2	1.762	1.781	21 B $(^4D)^6D^o$ + 18 C $(^5D)^6D^o$ + 9 C $(^5D)^4P^o$
41 557.08	40 752	3/2	1.655	1.496	20 B $(^4P)^6D^o$ + 12 B $(^6S)^6P^o$ + 8 C $(^5D)^6F^o$
41 843.85	41 743	7/2	1.190	1.302	18 B $(^4G)^6H^o$ + 8 B $(^6D)^6P^o$ + 7 B $(^4D)^4F^o$
42 254.19	42 499	3/2	1.578	1.489	14 B $(^6S)^4P^o$ + 11 B $(^4P)^6P^o$ + 7 C $(^5D)^4P^o$
43 044.02	42 997	5/2	1.449	1.446	8 B $(^4D)^4D^o$ + 7 B $(^4P)^6D^o$ + 7 B $(^4D)^4D^o$
43 341.85	43 340	3/2	0.975	1.032	17 B $(^4P)^6D^o$ + 9 B $(^2D)^4F^o$ + 9 B $(^4G)^4F^o$
43 815.01	43 937	7/2	1.348	1.388	14 B $(^6S)^6P^o$ + 14 B $(^4G)^6G^o$ + 8 A $(^5D)^6P^o$
43 949.98	43 852	5/2	1.385	1.567	19 B $(^4P)^6S^o$ + 13 B $(^4D)^6P^o$ + 5 A $(^5D)^4P^o$
45 876.34	45 974	3/2	1.384	1.555	14 B $(^4P)^6D^o$ + 9 C $(^5D)^6F^o$ + 8 B $(^4D)^6F^o$
45 937.18	46 049	7/2	1.298	1.282	11 B $(^6S)^6P^o$ + 8 B $(^4G)^6F^o$ + 6 C $(^3G)^4G^o$
46 112.24	46 223	5/2	1.405	1.345	20 B $(^4D)^6F^o$ + 12 B $(^4P)^6D^o$ + 11 B $(^4G)^6F^o$
46 352.99	46 392	7/2	1.271	1.274	15 B $(^4G)^6F^o$ + 13 B $(^4D)^6F^o$ + 7 B $(^4G)^6G^o$
46 509.40	46 476	5/2	1.371	1.528	17 B $(^6S)^4P^o$ + 8 B $(^4P)^6S^o$ + 7 B $(^6S)^6P^o$
46 649.42	46 573	5/2	1.334	1.304	15 B $(^4G)^6F^o$ + 8 C $(^5D)^6F^o$ + 7 B $(^4F)^6F^o$
46 733.38	46 680	3/2	1.858	1.796	18 B $(^4D)^6P^o$ + 16 B $(^4G)^6F^o$ + 14 B $(^4P)^6P^o$
47 101.61	46 984	5/2	0.893	0.864	14 B $(^2F)^4G^o$ + 13 B $(^4G)^4G^o$ + 10 C $(^3F)^4G^o$
47 358.36	47 365	7/2	1.151	1.076	14 B $(^2F)^4G^o$ + 14 B $(^4G)^4G^o$ + 8 C $(^3F)^4G^o$
47 970.82	47 875	5/2	1.169	1.287	11 B $(^4G)^6F^o$ + 9 C $(^5D)^6F^o$ + 7 B $(^4P)^6D^o$

Notes. [a]Klinkenberg et al. (1957).
[b]HFR+CPOL method: this work.
[c]First three major components are given in per cent. A, B, and C stand for $5d^66p$, $5d^56s6p$, and $5d^46s^26p$ configurations respectively.

compute the radiative parameters of highly excited atomic states accurately for this type of atomic structure.

By combining the theoretical branching fractions *BF* with the experimental lifetimes, the semi-empirical transition probabilities gA and oscillator strengths on a logarithmic scale log(gf) for 47 lines from 18 upper levels with the wavelength range of 204 to 441 nm were deduced and listed in Table 3. Two groups (Palmeri et al. 2006, Ortiz *& Mayo-García* 2012) had also reported gA and log(gf) of the 32 591.63 and 41 557.08 cm^{-1} levels, which are shown in the table for comparison. Note that *BF,* semi-empirical gA and log(gf) values

Table 3. Branching fractions, transition probabilities, oscillator strengths obtained in this work for 18 levels of Re I.

Upper level[a]		Lower level[a]				gA (10^6 s^{-1})[b]		log(gf)	
Assign.	E (cm^{-1}) Lifetime (ns)	Assign.	E (cm^{-1})	λ_{air} (nm)	BF	This work	Previous[c]	This work	Previous
$5d^4 6s^2(^5D)6p\ z\ ^6D^\circ_{3/2}$	32 591.63	$5d^5 6s^2\ a\ ^6S_{5/2}$	0.00	306.738	0.804	24.4 (C)	24.0	–1.47	–1.47[c], –1.38[d]
	$\tau = 132(8)$	$5d^5 6s^2\ a\ ^4P_{3/2}$	13 826.12	532.745	–	–	1.43	–	–2.22[c]
	–	$5d^6(^5D)6\ s\ a\ ^6D_{5/2}$	15 770.42	594.323	–	–	1.28	–	–2.17[c]
$5d^5 6s(^5P)6p\ y\ ^6D^\circ_{3/2}$	41 557.08	$5d^5 6s^2\ a\ ^6S_{5/2}$	0.00	240.56	0.669	84.1 (D+)	74.2	–1.12	–1.19[c]
	$\tau = 31.6(15)$	$5d^5 6s^2\ a\ ^4P_{5/2}$	11 583.96	333.536	–	–	2.55	–	–2.37[c]
	–	$5d^5 6s^2\ a\ ^4P_{3/2}$	13 826.12	360.505	–	–	1.88	–	–2.44[c]
	–	$5d^5 6s^2\ a\ ^4G_{5/2}$	14 621.46	371.15	–	–	3.44	–	–2.15[c]
	–	$5d^6(^5D)6\ s\ a\ ^6D_{3/2}$	16 327.51	396.248	–	–	5.02	–	–1.93[c]
	–	$5d^6(^5D)6\ s\ a\ ^6D_{1/2}$	17 238.30	441.089	0.150	18.9 (E)	16.7	–1.29	–1.37[c]
	–	$5d^5 6s^2\ a\ ^4D_{5/2}$	19 457.89	452.378	–	–	4.00	–	–1.91[c]
$418^\circ_{7/2}$	41 843.85	$5d^6(^5D)6\ s\ a\ ^6D_{9/2}$	11 754.52	332.248	0.664	68.7 (D+)	–	–0.95	–
	$\tau = 77.3(26)$	$5d^6(^5D)6\ s\ a\ ^6D_{5/2}$	15 770.42	383.423	0.149	15.4 (E)	–	– 1.47	–
$5d^5 6s(^5P)6p\ z\ ^4D^\circ_{3/2}$	42 254.19	$5d^5 6s^2\ a\ ^6S_{5/2}$	0.00	236.591	0.441	90.1 (D+)	–	– 1.12	–
	$\tau = 19.6(8)$	$5d^5 6s^2\ a\ ^4P_{5/2}$	11 583.96	325.955	0.236	48.1 (D)*	–	– 1.12*	–
	–	$5d^5 6s^2\ a\ ^4P_{3/2}$	13 826.12	351.664	0.148	30.3 (E)*	–	– 1.25*	–
$5d^5 6s(^5P)6p\ z\ ^4D^\circ_{5/2}$	43 044.02	$5d^6(^5D)6\ s\ a\ ^6D_{7/2}$	14 216.86	346.796	0.198	42.0 (E)	–	–1.12*	–
	$\tau = 28.3(8)$	–	–	–	–	–	–	–	–
$433^\circ_{3/2}$	43 341.85	$5d^5 6s^2\ a\ ^4G_{5/2}$	14 621.46	348.085	0.551	56.6 (D+)*	–	– 0.98*	–
	$\tau = 38.9(15)$	$5d^6(^5D)6\ s\ a\ ^6D_{1/2}$	17 238.30	382.981	0.210	21.6 (D+)*	–	– 1.32*	–
$438^\circ_{7/2}$	43 815.01	$5d^5 6s^2\ a\ ^6S_{5/2}$	0.00	228.162	0.648	274 (C)	–	– 0.67	–
	$\tau = 18.9(7)$	$5d^6(^5D)6\ s\ a\ ^6D_{9/2}$	11 754.52	311.820	0.234	98.9 (D+)	–	– 0.85	–
$439^\circ_{5/2}$	43 949.98	$5d^5 6s^2\ a\ ^6S_{5/2}$	0.00	227.461	0.180	109 (E)	–	– 1.07	–
	$\tau = 9.9(7)$	$5d^6(^5D)6\ s\ a\ ^6D_{7/2}$	14 216.86	336.228	0.373	226 (D)	–	– 0.42	–
	–	$5d^5 6s^2\ a\ ^4G_{5/2}$	14 621.46	340.867	0.159	96.3 (E)	–	– 0.77	–
$458^\circ_{3/2}$	45 876.34	$5d^5 6s^2\ a\ ^6S_{5/2}$	0.00	217.909	0.753	78.9 (C)	–	–1.25	–
	$\tau = 38.2(16)$	–	–	–	–	–	–	–	–
$459^\circ_{7/2}$	45 937.18	$5d^5 6s^2\ a\ ^6S_{5/2}$	0.00	217.621	0.724	460 (C)	–	– 0.49	–
	$\tau = 12.6(10)$	–	–	–	–	–	–	–	–
$461^\circ_{5/2}$	46 112.24	$5d^5 6s^2\ a\ ^6S_{5/2}$	0.00	216.794	0.526	304 (D+)	–	– 0.67	–
	$\tau = 10.4(6)$	$5d^5 6s^2\ a\ ^4G_{5/2}$	14 621.46	317.461	0.210	121(D+)	–	–0.74	–
$463^\circ_{7/2}$	46 352.99	$5d^5 6s^2\ a\ ^6S_{5/2}$	0.00	215.668	0.275	103 (D+)	–	– 1.14	–
	$\tau = 21.4(9)$	$5d^6(^5D)6\ s\ a\ ^6D_{7/2}$	14 216.86	311.086	0.411	154 (D+)	–	– 0.65	–
	–	$5d^6(^5D)6\ s\ a\ ^6D_{5/2}$	15 770.42	326.89	0.116	43.3 (E)	–	– 1.16	–
$465^\circ_{5/2}$	46 509.40	$5d^5 6s^2\ a\ ^6S_{5/2}$	0.00	214.942	0.455	133 (D+)	–	– 1.03	–
	$\tau = 20.5(10)$	$5d^5 6s^2\ a\ ^4G_{7/2}$	15 058.19	317.861	0.123	35.9 (E)	–	– 1.26	–
	–	$5d^5 6s^2\ a\ ^4D_{7/2}$	17 330.82	342.619	0.205	60.1 (D+)	–	– 0.97	–
$466^\circ_{5/2}$	46 649.42	$5d^5 6s^2\ a\ ^6S_{5/2}$	0.00	214.297	0.326	124 (D)	–	– 1.06	–
	$\tau = 15.7(9)$	$5d^6(^5D)6\ s\ a\ ^6D_{7/2}$	14 216.86	308.242	0.476	182 (D+)	–	– 0.58	–
$467^\circ_{3/2}$	46 733.38	$5d^5 6s^2\ a\ ^6S_{5/2}$	0.00	213.913	0.611	136 (C)	–	– 1.03	–
	$\tau = 18.0(6)$	$5d^6(^5D)6\ s\ a\ ^6D_{3/2}$	16 327.51	328.789	0.165	36.6 (E)	–	– 1.23	–
$471^\circ_{5/2}$	47 101.61	$5d^5 6s^2\ a\ ^4P_{5/2}$	11 583.96	281.467	0.183	67.7 (E)*	–	– 1.09*	–
	$\tau = 16.2(6)$	$5d^6(^5D)6\ s\ a\ ^6D_{7/2}$	14 216.86	304.004	0.161	59.6 (E)	–	– 1.08	–
	–	$5d^6(^5D)6\ s\ a\ ^6D_{5/2}$	15 770.42	319.079	0.128	47.4 (E)*	–	– 1.14*	–
	–	$5d^6(^5D)6\ s\ a\ ^6D_{3/2}$	16 327.51	324.855	0.115	42.6 (E)*	–	– 1.17*	–
	–	$5d^5 6s^2\ a\ ^4D_{7/2}$	17 330.82	335.804	0.122	45.4 (E)*	–	– 1.11*	–
$473^\circ_{7/2}$	47 358.36	$5d^5 6s^2\ a\ ^6S_{5/2}$	0.00	211.089	0.493	94.9 (D+)	–	– 1.20	–
	$\tau = 41.6(17)$	$5d^5 6s^2\ a\ ^4G_{7/2}$	15 058.19	309.506	0.150	28.8 (E)*	–	– 1.38*	–
$479^\circ_{5/2}$	47 970.82	$5d^5 6s^2\ a\ ^4G_{5/2}$	14 621.46	299.769	0.387	94.8 (E)	–	– 0.89	–

Table 3 – *continued*

Upper level[a] Assign.	E (cm^{-1}) Lifetime (ns)	Lower level[a] Assign.	E (cm^{-1})	λ_{air} (nm)	BF	gA (10^6 s^{-1})[b] This work	Previous[c]	log(gf) This work	Previous
	τ = 24.5(25)	5d^6(^{5}D)6 s a ^{6}D$_{5/2}$	15 770.42	310.465	0.171	42.0 (E)*	–	− 1.22*	–
	–	5d^6(^{5}D)6 s a ^{6}D$_{3/2}$	16 327.51	315.932	0.163	39.9 (E)*	–	− 1.22*	–

Notes. [a]Kramida et al. (2018).
[b]gA- and log gf-values obtained in this work were deduced from the combination of HFR+CPOL branching fractions with experimental lifetimes. The estimated uncertainties are given between parentheses. They are indicated by the same code letter as the one used in the NIST data base (Kramida et al. 2018), i.e. C (≤ 25 per cent), D+ (≤ 40 per cent), D (≤ 50 per cent), and E (> 50 per cent) (see the text).
[c]Semi-empirical values by Palmeri et al. (2006).
[d]Measured values by Ortiz and Mayo-García (2012).
*Affected by strong cancellation effects on the line strength (cancellation factor, CF, less than 0.05) (Cowan, 1981).

obtained in this work are only given for transitions with a branching fraction larger than 0.1. Actually, most of the weaker branches are affected by strong cancellation effects, i.e. with CF < 0.05. The presently reported semi-empirical transition probabilities and oscillator strengths that are still affected by strong cancellation effects are marked by an asterisk. The errors on the radiative rates (gA) shown in this table were determined from the present BF values using the same estimate made in Ba I by Wang et al. (2019), i.e. 20, 30, 35, 40, and 55 per cent for BF = 0.8–1.0, 0.6–0.8, 0.4–0.6, 0.2–0.4, and 0.1–0.2, respectively. We therefore assume that the rescaling of the transition probabilities using the measured lifetimes completely corrects the errors due to our calculated lifetimes and that the errors affecting our branching fractions are the same as those determined in Ba I (Wang et al. 2019).

In summary, radiative lifetimes for 19 odd-parity levels of Re I with energy range of 32 591.63 to 47 970.82 cm^{-1} were determined by the TR-LIF method, and as far as we know, 15 of them are reported for the first time. Branching fractions for 47 lines from 18 levels were computed using the HFR+CPOL model, based on which the semi-empirical transition probabilities and oscillator strengths for these lines were obtained by combining the lifetime results measured in this work.

ACKNOWLEDGEMENTS

This work was supported by the National Natural Science Foundation of China (Grant No. U1832114) and, Science and Technology Development Planning Project of Jilin Province (Grant No. 20180101239JC). PP and PQ are respectively Research Associate and Research Director of the Belgian F.R.S.-FNRS from which financial support is gratefully acknowledged.

REFERENCES

Blume M., Watson R. E., 1962, Proc. R. Soc. Lond. A, 270, 127
Blume M., Watson R. E., 1963, Proc. R. Soc. Lond. A, 271, 565
Corliss C. H., Bozman W. R., 1962, Experimental Transition Probabilities for Spectral Lines of Seventy Elements. U.S. GPO, Washington, DC, p. 305
Cowan R. D., 1981, The Theory of Atomic Structure and Spectra. University of California Press, Berkeley
Duquette D. W., Salih S., Lawler J. E., 1982, J. Phys. B: At. Mol. Phys., 15, L897
Fivet V., Palmeri P., Quinet P., Biémont É., Xu H. L., Svanberg S., 2006a, Eur. Phys. J. D, 37, 29
Fivet V., Quinet P., Biémont É., Xu H. L., 2006b, J. Phys. B: At. Mol. Opt. Phys., 39, 3587
Fraga S., Karwowski J., Saxena K. M. S., 1976, Handbook of Atomic Data. Elsevier, Amsterdam
Guthrie B. N. G., 1972, Astrophys. Space Sci., 15, 214
Jaschek M., Brandi E., 1972, A&A, 20, 233
Klinkenberg P. F. A., Meggers W. F., Velasco R., Catalán M. A., 1957, J. Res. Natl. Bur. Stand., 59, 319
Kramida A., Ralchenko Y., Reader J., NIST ASD Team, 2018, NIST Atomic Spectra Database 5.6.1. National Institute of Standards and Technology, Gaithersburg, MD. Available at: https://physics.nist.gov/asd
Li Q., Yu Q., Li Y. F., Wang Q., Yang Y., Dai Z. W., 2019, Phys. Scr., 94, 075405
Moore C. E., 1958, Atomic Energy Levels, U.S. GPO, Washington, DC, p. 165
Ortiz M., Mayo-García R., 2012, J. Phys. B: At. Mol. Opt. Phys., 45, 055701
Palmeri P., Quinet P., Biémont É., Svanberg S., Xu H. L., 2006, Phys. Scr., 74, 297
Quinet P., Fivet V., Palmeri P., Biémont É., Engström L., Lundberg H., Nilsson H., 2009, A&A, 493, 711
Quinet P., Palmeri P., Biémont É., Jorissen A., Van Eck S., Svanberg S., Xu H. L., P lez B., 2006, A&A, 448, 1207
Quinet P., Palmeri P., Biémont É., Li Z. S., Zhang Z. G., Svanberg S., 2002, J. Alloys Compd., 344, 255
Quinet P., Palmeri P., Biémont É., McCurdy M. M., Rieger G., Pinnington E. H., Wickliffe M. E., Lawler J. E., 1999, MNRAS, 307, 934
Shang X., Tian Y. S., Wang Q., Fan S., Bai W. S., Dai Z. W., 2014, MNRAS, 442, 138
Shang X., Wang Q., Zhang F. F., Wang C., Dai Z. W., 2015, JQSRT, 163, 34
Tian Y. S., Wang X. H., Yu Q., Li Y. F., Gao Y., Dai Z. W., 2016, MNRAS, 457, 1393
Wang Q., Gamrath S., Palmeri P., Quinet P., Yu Q., Zhang M. Q., Dai Z. W., 2019, J. Quant. Spectrosc. Radiat. Transfer, 225, 35
Wickliffe M. E., Lawler J. E., Nave G., 2000, J. Quant. Spectrosc. Radiat. Transfer, 66, 363
Wyart J. F., 1978, Phys. Scr., 18, 87
Zhang M. Q., Zhou L. N., Gao Y., Yu Q., Wang X. H., Wang Q., Gong Y. M., Dai Z. W., 2018, J. Phys. B: At. Mol. Opt. Phys., 51, 205001
Zhang W., Feng Y. Y., Dai Z. W., 2010, J. Opt. Soc. Am. B, 27, 2255
Zhang W., Feng Y. Y., Jiang L. Y., Du S., Wang L., Jiang Z., Dai Z. W., 2011, J. Phys. B: At. Mol. Opt. Phys., 44, 175002
Zhou L. N., Gamrath S., Palmeri P., Quinet P., Zhang M. Q., Dai Z. W., 2018, ApJ, 238, 3

This paper has been typeset from a Microsoft Word file prepared by the author.